International Journal of Robotics and Control Systems
Vol. 5, No. 5, 2025, pp. 2508-2521
ISSN 2775-2658
http://pubs2.ascee.org/index.php/ijrcs

Integration of Fuzzy-PI with STA–NTSMC: A Novel Hybrid Control Approach for Induction Motor Drives

An Khuong Nguyen [a,1], Ngoc Thuy Pham [b,2*]

[a,b] Dept. of Electrical Engineering Technology, Industrial University of Ho Chi Minh City, Ho Chi Minh City 700000, Vietnam
[1] Khuong@cantab.net; [2] ngocpham1020@gmail.com
*Corresponding Author

ARTICLE INFO

Article history
Received September 17, 2025
Revised October 04, 2025
Accepted November 19, 2025

Keywords
Induction Motor Drives;
Fuzzy-PI Control;
Super-Twisting Algorithm;
Field Oriented Control;
Robust Control

ABSTRACT

This paper presents a novel fuzzy-PI integrated super-twisting nonsingular terminal sliding mode control (FPI–STANTSMC) strategy for high-performance induction motor drives. In the proposed scheme, a fuzzy-PI regulator adaptively tunes the proportional–integral gains in real time, enhancing steady-state accuracy and robustness against parameter uncertainties. The super-twisting algorithm (STA) generates a continuous control vector to mitigate chattering, while the nonsingular terminal sliding-mode control (NTSMC) surface guarantees finite-time convergence without singularities. Closed-loop stability is established through Lyapunov analysis. The controller is validated in MATLAB/Simulink under challenging scenarios, including wide-range bidirectional speed transitions, sudden load disturbances, and severe stator/rotor resistance variations. Comparative evaluations demonstrate that the proposed FPI–STANTSMC outperforms PI, fuzzy-PI, and PI-FOSMC controllers, with a reduction in rise time of about 41% relative to PI, 20% to PI-FOSMC, and 8% to fuzzy-PI. Overshoot is eliminated, whereas PI, fuzzy-PI, and PI-FOSMC exhibit overshoots of 1.8 rad/s, 0.8 rad/s, and 0.4 rad/s, respectively. Under rated load, the proposed scheme maintains near-zero steady-state error compared to 1 rad/s for PI and fuzzy-PI, 0.5 rad/s for PI-FOSMC, while preserving smooth electromagnetic torque with substantially reduced chattering. These results confirm the proposed strategy as a robust and practical solution for high-performance IM drives.

1. Introduction

Induction motor (IM) drives are extensively employed in industrial automation, transportation, and renewable energy systems due to their rugged construction, high efficiency, and low cost [1], [2]. However, achieving high-performance speed regulation remains a challenge because IMs are nonlinear and multivariable systems whose dynamics are affected by parameter variations, load disturbances, and unmodeled nonlinearities [3], [4].

Conventional proportional–integral (PI) controllers are popular in practice thanks to their simplicity and ease of implementation [5], [6]. Nevertheless, they exhibit poor robustness, degraded

steady-state accuracy under load changes, and limited adaptability across wide operating ranges. Intelligent variants such as fuzzy-PI [7]–[16] and neural-network-based PI controllers [17]–[28] improve adaptability, but they still lack guaranteed robustness and stability in highly uncertain conditions.

Sliding-mode control (SMC) is well known for its robustness against uncertainties [29]–[34], yet the first-order version suffers from severe chattering [35], [36]. Higher-order methods have therefore been proposed [37]–[54]. The super-twisting algorithm (STA) reduces chattering with continuous control signals, and nonsingular terminal SMC (NTSMC) achieves finite-time convergence without singularities. Although fuzzy logic, STA, and NTSMC have been combined with SMC in various contexts [55]–[58], existing approaches usually focus on either adaptability or robustness in isolation, rather than providing an integrated solution. Importantly, the application of fuzzy-PI tuning within a hybrid STA–NTSMC framework for IM drives has not been reported to date.

Compared to neural networks or fuzzy-SMC approaches, fuzzy-PI tuning is computationally efficient, interpretable, and easy to implement online, making it highly suitable for real-time motor drive applications. Its integration with STA–NTSMC offers the potential to simultaneously deliver adaptive gain regulation, reduced chattering, and finite-time convergence.

The research contribution of this paper is the first integration of a fuzzy-PI regulator with a STA–NTSMC hybrid control scheme for induction motor drives. Specifically, (i) the fuzzy-PI regulator adaptively adjusts PI gains online to improve steady-state accuracy under parameter uncertainties, (ii) the STA generates continuous control vector to suppress chattering, and (iii) the NTSMC ensures finite-time convergence without singularities. Stability is analyzed using Lyapunov theory, and the controller is validated under wide speed transitions, load disturbances, and parameter variations. Comparative simulations confirm significant improvements in rise time, settling time, overshoot, steady-state error, and torque ripple compared with PI, fuzzy-PI, and PI-FOSMC controllers.

The remainder of this paper is organized as follows: Section 2 presents the mathematical modeling of the IM system. Section 3 details the design of the proposed FPI–STANTSMC controller and stability analysis using Lyapunov theory. Section 4 reports simulation results and comparative performance evaluation. Finally, Section 5 concludes the paper and outlines potential future research directions.

2. Mathematical Model of Induction Motor Drives

This section presents the mathematical formulation of the IM in a synchronously rotating reference frame, which enables torque–flux decoupling and serves as the foundation for FOC design [59], [60]. The corresponding state–space representation is expressed as follows:

$$\dot{x}(t)=\mathrm{A}x(t)+Bu(t) \tag{1}$$

where: x, A, B and u can be defined as:

$$x(t)=[i_{s\alpha}\quad i_{s\beta}\quad \varphi_{r\alpha}\quad \varphi_{r\beta}\quad \omega_r]^T;\quad u(t)=[u_{s\alpha}\quad u_{s\beta}\quad T_L]^T$$

$$A=\begin{bmatrix} a_{11} & 0 & a_{13} & a_{14} & a_{15} \\ 0 & a_{11} & -a_{14} & a_{13} & a_{25} \\ \frac{L_m}{\tau_r} & 0 & \frac{-1}{\tau_r} & \omega_r & \varphi_{r\beta} \\ 0 & \frac{L_m}{\tau_r} & -\omega_r & \frac{-1}{\tau_r} & -\varphi_{r\alpha} \\ -b\varphi_{r\beta} & b\varphi_{r\alpha} & bi_{s\beta} & -bi_{s\alpha} & \left(\frac{-B}{J}\right) \end{bmatrix};\quad B=\begin{bmatrix} \frac{1}{\sigma L_s} & 0 & 0 \\ 0 & \frac{1}{\sigma L_s} & 0 \\ 0 & 0 & 0 \\ 0 & 0 & 0 \\ 0 & 0 & \frac{-1}{J} \end{bmatrix}$$

with $i_{s\alpha}$; $i_{s\beta}$; $u_{s\alpha}$; $u_{s\beta}$; $\varphi_{r\alpha}$; $\varphi_{r\beta}$ are components of the stator's current, stator's voltage and rotor's flux in the $\alpha\beta$ reference frame. T_L is the load torque.

$$\tau_r = \frac{L_r}{R_r};\ \sigma = 1 - \frac{L_m^2}{L_r L_s};\ \gamma = \frac{L_m}{L_r};\ k = \frac{3pL_m}{2L_r};\ b = \frac{k}{J}$$

$$a_{11} = -\frac{1}{\sigma L_s}\left(R_s + \frac{L_m^2}{L_r \tau_r}\right);\ a_{13} = \frac{\gamma}{\sigma L_s \tau_r};\ a_{14} = -\frac{\gamma}{\sigma L_s}\omega_r;\ a_{15} = -\frac{\gamma}{\sigma L_s}\varphi_{r\beta};\ a_{25} = \frac{\gamma}{\sigma L_s}\varphi_{r\alpha}$$

L_s, L_r: Stator and rotor inductances; L_m: Mutual inductance; R_s, R_r: Stator and rotor resistances; J: the inertia of motor and load; σ: Total linkage coefficient; p: Number of pole pairs; τ_r: Rotor time constant; ω_r: Rotor speed. Based on the dynamics of induction motor in stator fixed reference frame, the stator flux can be estimated such as:

$$\begin{cases} \varphi_{s\alpha} = \int_0^t (u_{s\alpha} - R_s i_{s\alpha})dt \\ \varphi_{s\beta} = \int_0^t (u_{s\beta} - R_s i_{s\beta})dt \end{cases} \quad (2)$$

The stator and rotor flux linkage phase is given by (3):

$$\varphi_s = \sqrt{\varphi_{s\alpha}^2 + \varphi_{s\beta}^2};\quad \varphi_r \approx \frac{L_m}{L_r}\varphi_s \quad (3)$$

Torque can be calculated such as:

$$T_e = \frac{3}{2}p\left(i_{s\beta}\varphi_{s\alpha} - i_{s\alpha}\varphi_{s\beta}\right) \quad (4)$$

The mechanical dynamics follow:

$$J\frac{d\omega_r}{dt} = T_e - T_L - B\omega_r \quad (5)$$

The derived state–space model provides the foundation for the subsequent control design aimed at improving drive performance.

3. Novel Hybrid Fuzzy-PI–STA–NTSMC control structure for IMDs

Based on the proposed FPI-STANTSMC control strategy, the tracking errors are defined as follows:

$$\begin{aligned} e(t) &= \omega_r^*(t) - \omega_r(t) \\ \dot{e}(t) &= \dot{\omega}_r^*(t) - \dot{\omega}_r(t) \end{aligned} \quad (6)$$

To guarantee finite-time convergence and avoid singularities, the proposed sliding surface is defined as:

$$s(t) = e(t) + \alpha|e|^{p/q} sat\left(\frac{e}{\phi}\right);\quad With:\ \alpha > 0;\ \phi > 0\ \&\ 0 < \frac{p}{q} < 1 \quad (7)$$

The derivative of the sliding surface is given by:

$$\dot{s}(t) = \dot{e}(t) + \alpha\frac{p}{q}|e|^{(p/q)-1}sat\left(\frac{e}{\phi}\right) + \alpha|e|^{(p/q)}\frac{d}{dt}\left[sat\left(\frac{e}{\phi}\right)\right] \quad (8)$$

The Lyapunov function is selected as:

$$V(t) = \frac{1}{2}s^2(t) \quad (9)$$

Its derivative can obtain:

$$\frac{dV(t)}{dt} = s(t)\dot{s}(t) \quad (10)$$

To satisfy: $\frac{dV(t)}{dt} < 0$Then: $s(t)\dot{s}(t) < 0$ From equation (8), a hybrid FPI–STANTSMC control law is designed as follows:

$$\dot{s}(t) = -\beta u(t) = -\beta[u_{FPI}(t) + u_{STANTSMC}(t)] \quad (11)$$

$$u_{FPI}(t) = K_{FP}(t)e(t) + K_{FI}(t)\int_0^t e(t)dt \quad (12)$$

$$u_{STA\_NTSMC}(t) = \phi\big(s(t)\big) + v(t)$$

$$where \quad \begin{cases} \phi\big(s(t)\big) = k_\alpha|s(t)|^{1/2}sat\left(\frac{s(t)}{\phi}\right) \\ v(t) = k_\beta\int_0^t sat\left(\frac{s(t)}{\phi}\right)dt \end{cases} \quad with:\ k_\alpha > 0;\ k_\beta > 0;\ \phi > 0 \quad (13)$$

Combining equation (5), (6), (8), (11) and substituting the IM dynamics into the sliding condition the virtual control vector isq is designed as follows:

$$i_{sq}^* = \frac{2L_r}{3pL_m\varphi_r}\{J\dot{\omega}_r^* + B\omega_r^* + T_L + \beta u(t)\} \quad with\ \beta\ is\ positive\ constant \quad (14)$$

The final control law is obtained by the direct superposition of the fuzzy-PI and STA–NTSMC components. Since the fuzzy-PI output primarily compensates for steady-state errors through adaptive gain tuning, and the STA–NTSMC output governs transient dynamics and robustness, their contributions are complementary rather than conflicting. The fuzzy-PI action has relatively low bandwidth and dominates steady-state regulation, whereas the STA–NTSMC term ensures fast dynamic response and disturbance rejection. A normalization and weighting strategy ensures complementary operation rather than redundancy. Therefore, this design avoids redundancy and ensures smooth cooperation between the two control signals.

Combining formulas (10), (11), (12) and (13) we get:

$$\frac{dV(t)}{dt} = s(t)\dot{s}(t) = -\beta s(t)[u_{FPI}(t) + u_{STANTSMC}(t)] \quad (15)$$

If $e(t) > 0$, from equation (7) we have $s(t) > 0$, combining equation (11), (12), (13) we have $\dot{s}(t) < 0$. Therefore $\frac{dV(t)}{dt} = s(t)\dot{s}(t) < 0$

If $e(t) < 0$, from equation (7) we have $s(t) < 0$, combining equation (11), (12), (13) we have $\dot{s}(t) > 0$. Therefore $\frac{dV(t)}{dt} = s(t)\dot{s}(t) < 0$

From equation (15) we have: $\frac{dV(t)}{dt} = s(t)\dot{s}(t) = -\beta s(t)[u_{FPI}(t) + u_{STANTSMC}(t)] < 0 \forall e(t)$

Thus, the system is always stable according to Lyapunov stability theory.

In the proposed strategy, the conventional PI regulator is replaced with a FPI controller to enhance adaptability and steady-state accuracy under varying operating conditions. The FPI controller function is designed as in (12). Where, $K_{FP}(t)$ and $K_{FI}(t)$ are the proportional and integral gains, respectively. Unlike the fixed-gain PI, the FPI employs a fuzzy inference system (FIS) to adaptively adjust $K_{FP}(t)$ and $K_{FI}(t)$ in real time. The inputs to the FPI are defined as: $e(t) = \omega_r^*(t) - \omega_r(t)$ and $\Delta e(t) = e(k) - e(k-1)$ corresponding to the instantaneous speed error and its variation. The fuzzy inference system employs triangular membership functions for both inputs, defined over the range [−1,1] with linguistic variables {NB, NM, NS, Z, PS, PM, PB (Negative Big → Positive Big)} as in Fig. 1. The fuzzy rule base is constructed to provide a self-tuning mechanism are presented in Table 1.

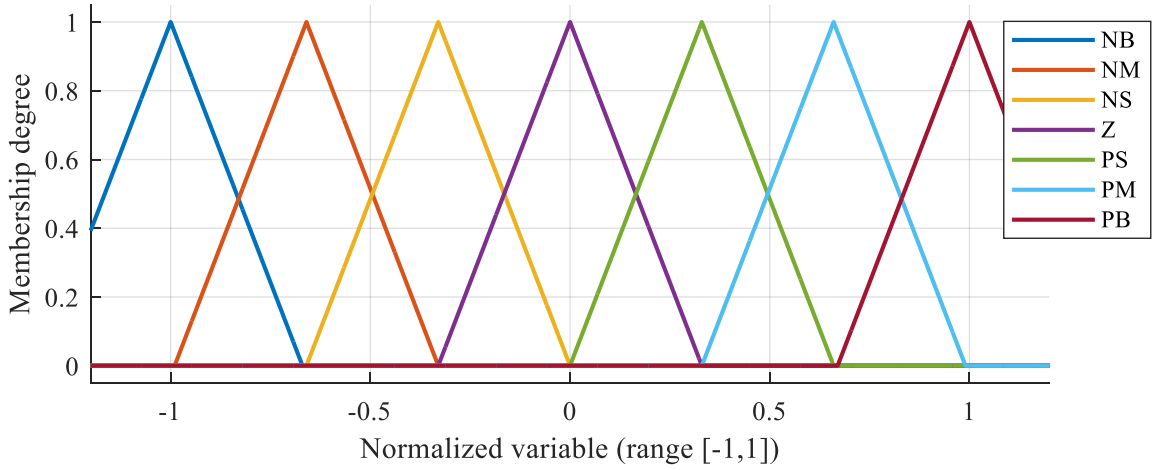

Fig. 1. Triangular membership functions for inputs

Table 1. Fuzzy rule base (ΔKp / ΔKi)

e(t)/Δe(t)	NB	NM	NS	Z	PS	PM	PB
NB	NB/Z	NB/NS	NB/NM	NB/NB	NM/NB	NS/NB	Z/NB
NM	NB/PS	NB/Z	NB/NS	NM/NM	NS/NB	Z/NB	PS/NB
NS	NB/PM	NB/PS	NM/Z	NS/NS	Z/NM	PS/NB	PM/NB
Z	NB/PB	NM/PM	NS/PS	Z/Z	PS/NS	PM/NM	PB/NB
PS	NM/PB	NS/PB	Z/PM	PS/PS	PM/Z	PB/NS	PB/NM
PM	NS/PB	Z/PB	PS/PB	PM/PM	PB/PS	PB/Z	PB/NS
PB	Z/PB	PS/PB	PM/PB	PB/PB	PB/PM	PB/PS	PB/Z

The mapping from inputs to gains is formally represented as:

$$\begin{bmatrix} K_{FP(t)} \\ K_{FI(t)} \end{bmatrix} = F\big(e(t), \Delta e(t)\big) \tag{16}$$

where $F\big(e(t), \Delta e(t)\big)$denotes the nonlinear fuzzy mapping defined by a rule base and membership functions. A Mamdani-type FIS with triangular membership functions, min–max inference, and centroid defuzzification is adopted for computational simplicity and real-time applicability. The block diagram of Fuzzy-PI Regulator is shown in Fig. 2, whereas the block diagram of Novel Hybrid FPI–STANTSMC control structure for IMDs is shown in Fig. 3.

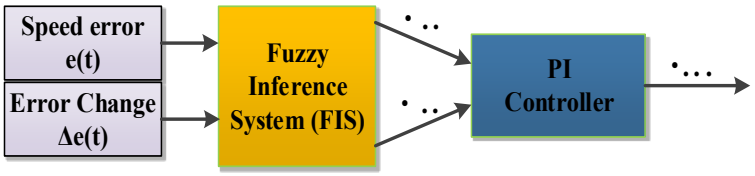

Fig. 2. The block diagram of Fuzzy-PI Regulator

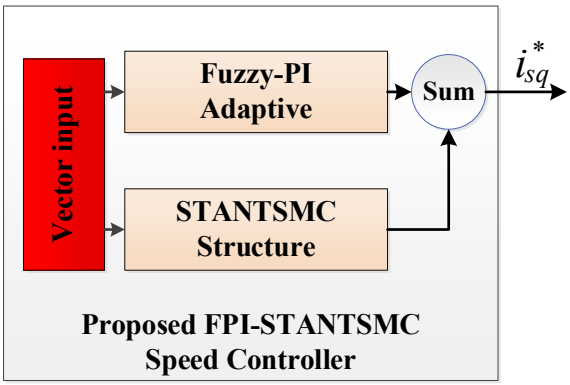

Fig. 3. Novel Hybrid FPI–STANTSMC control structure

4. Simulation Results and Discussion

The performance of the proposed Fuzzy-PI–STA–NTSMC controller was evaluated through simulations in MATLAB/Simulink 2023b on a squirrel-cage IM model. The IM under study is rated at 400 V, 50 Hz, two poles, and 2880 rpm. The machine parameters are: Rs = 1.97 Ω, Rr = 1.96 Ω, Ls = 0.0154 H, Lr = 0.0154 H, Lm = 0.3585H, J = 0.00242 kg.m2, B=0.0005. The overall simulation framework is illustrated in Fig. 4.

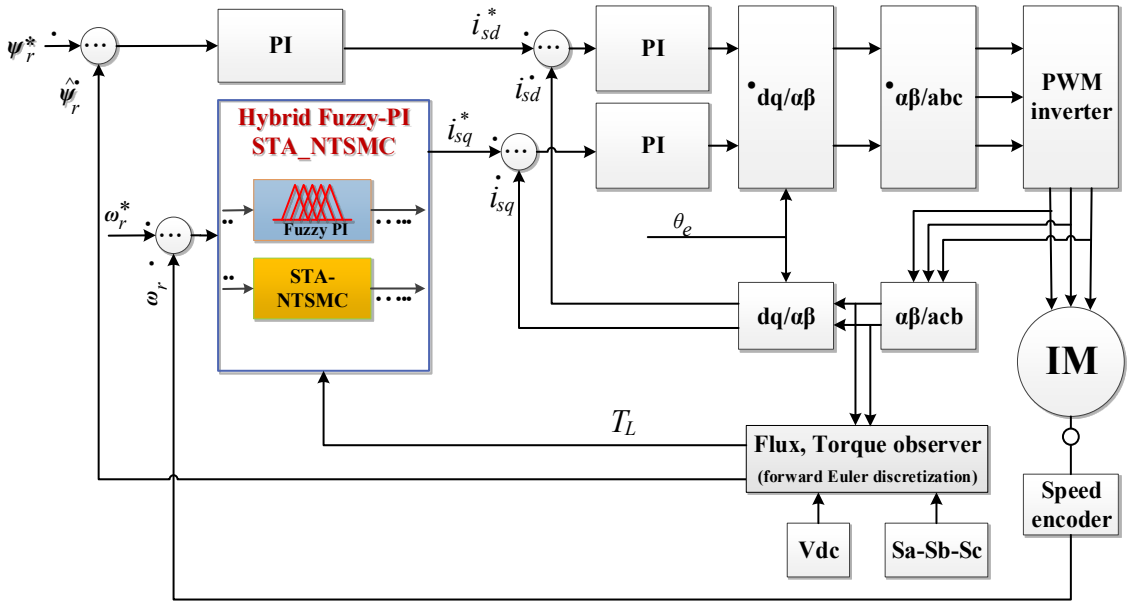

Fig. 4. Diagram of Fuzzy-PI–STA–NTSMC vector control for IM drives

4.1. Dynamic Performance Evaluation under Rated Load Moment

Fig. 5 illustrates the dynamic performance of the induction motor drive under variable-speed operation at ±300 rad/s, –100 rad/s, and 180 rad/s with a rated load torque of 7 Nm. The proposed

FPI–STANTSMC controller is compared with the conventional PI, fuzzy-PI, and PI-FOSMC schemes. During the start-up condition, the proposed controller achieves the fastest response, reaching a settling time of approximately 0.04 s, while PI, fuzzy-PI, and PI-FOSMC require 0.07 s, 0.045 s, and 0.055 s, respectively (Table 2). Overshoot is practically negligible, remaining at 0.5%, whereas PI and fuzzy-PI display overshoots of about 5% and 3%. These results confirm that the proposed hybrid design enables smoother and more precise acceleration compared with existing controllers. When a rated torque of 7 Nm is suddenly applied at 0.3 s, the proposed scheme limits the transient speed dip to less than 3.5 rad/s and restores the reference within 0.005 s, with a steady-state error of only 0.1 rad/s. By contrast, PI and fuzzy-PI exhibit larger deviations of approximately 1 rad/s with slower or indeterminate recovery, while PI-FOSMC shows better robustness but introduces noticeable chattering. The proposed method effectively eliminates this drawback by ensuring both fast recovery and smooth control. Under speed reversal from +300 rad/s to –300 rad/s, the proposed controller again demonstrates superior behavior, maintaining overshoot below 2% and settling in about 0.04 s. In comparison, PI and fuzzy-PI produce larger overshoots of around 8% and 5%, along with longer convergence times, while PI-FOSMC performs moderately better but still fails to achieve the precision and smoothness of the proposed strategy.

In the broader context of recent literature, Fuzzy–STA [55] has proven effective in reducing chattering, but it does not adequately address steady-state accuracy. Conversely, adaptive NTSMC [57] ensures finite-time convergence, yet it lacks the PI-type fuzzy adaptation that is particularly beneficial for induction motor drives. The novelty of this work lies in unifying fuzzy-PI adaptation, STA-based chattering suppression, and NTSMC finite-time convergence within a single framework specifically validated for IM drives. This integration simultaneously addresses adaptability, robustness, and precision, as confirmed by the simulation outcomes in Fig. 5 and Table 2.

Table 2. Performance comparison under variable-speed operation

Controller	Settling time (s)	Overshoot (%)	Steady-state error (rad/s)
PI	0.07	5	1
Fuzzy-PI	0.045	3	1
PI-FOSMC	0.055	2.5	0.4
FPI-STANTSMC	0.04	0.5	0.1

The overall quantitative comparison in Table 2 highlights that the proposed controller consistently achieves the lowest settling time, the smallest overshoot, and the least steady-state error among all tested schemes. These improvements validate its ability to combine fast dynamics with robust steady-state accuracy, while also avoiding the steady-state oscillations observed in PI-FOSMC.

4.2. Robustness Evaluation under Load Disturbance

Fig. 6 evaluates the performance of the IM drive system under multiple load disturbances at low (+20 rad/s), high (260 rad/s), and medium (150 rad/s) speed ranges, where the rated load torque of 7 Nm is switched on and off. The detailed responses in Zoom 1, Zoom 2, and Zoom 3 demonstrate that the proposed FPI–STANTSMC controller provides superior robustness compared to the conventional PI, Fuzzy-PI, and PI-FOSMC controllers. Specifically, the proposed scheme achieves (i) the fastest disturbance rejection, (ii) the smallest transient overshoot during large speed/torque variations, and (iii) the lowest steady-state error following the disturbance.

Although torque spikes are observed for all controllers due to the imposed load changes, the proposed method effectively damps the oscillations within the shortest time, thereby reducing mechanical stress and enhancing overall drive stability. Quantitative observations confirm that the proposed controller reduces peak speed deviation and settling time by a significant margin. These improvements highlight the effectiveness and practicality of the combined Fuzzy-PI and STA_NTSMC structure in achieving robust disturbance rejection for high-performance IM drives.

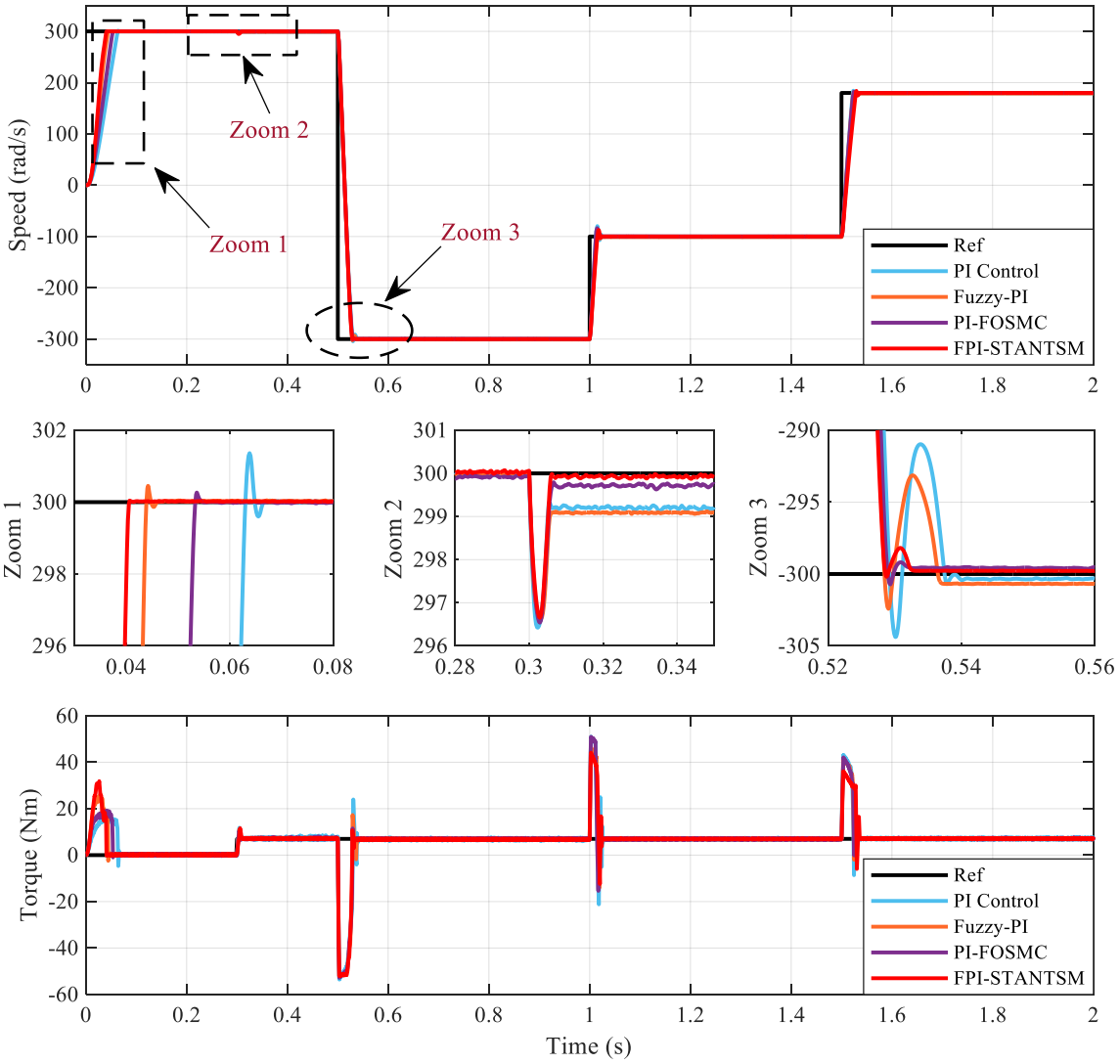

Fig. 5. Performance of PI, Fuzzy-PI, PI-FOSMC and FPI-STANTSMC under the variable speed

4.3. Robustness Evaluation under Parameter Variations (Resistance Changes)

Fig. 7 investigates the robustness of the IM drive under parameter variations, where both rotor and stator resistances are increased by 200% under different speed ranges with rated load torque. From the speed response (top plots, Zoom 1), the proposed FPI–STANTSMC controller achieves the most accurate tracking under resistance uncertainty. PI and Fuzzy-PI controllers exhibit slower convergence and larger steady-state deviations (≈5–10 rad/s). PI-FOSMC improves tracking accuracy but still produces residual oscillations. In contrast, the proposed controller maintains negligible error (<1 rad/s) with the fastest settling time. In the torque response (middle plots, Zoom 2), all controllers experience spikes due to sudden resistance variation. However, the proposed controller damps the oscillations much faster, thereby reducing torque ripple and mechanical stress. PI and Fuzzy-PI show sustained oscillations, while PI-FOSMC still suffers from moderate chattering. An important observation is that the FPI–STANTSMC effectively suppresses chattering compared to PI-FOSMC. Although FOSMC enhances robustness, its discontinuous control inherently induces steady-state oscillations, as observed in Zoom 2. By contrast, the NTSMC formulation combined with the Super-Twisting Algorithm (STA) ensures continuous control action, eliminating high-frequency oscillations while preserving fast convergence.

Overall, the results confirm that the FPI–STANTSMC controller provides superior robustness against parameter variations, combining fast recovery, low overshoot, and minimal steady-state error. This validates its effectiveness not only under load disturbances (Section 4.2) but also under severe parameter uncertainties, ensuring reliable IM drive performance in practical applications.

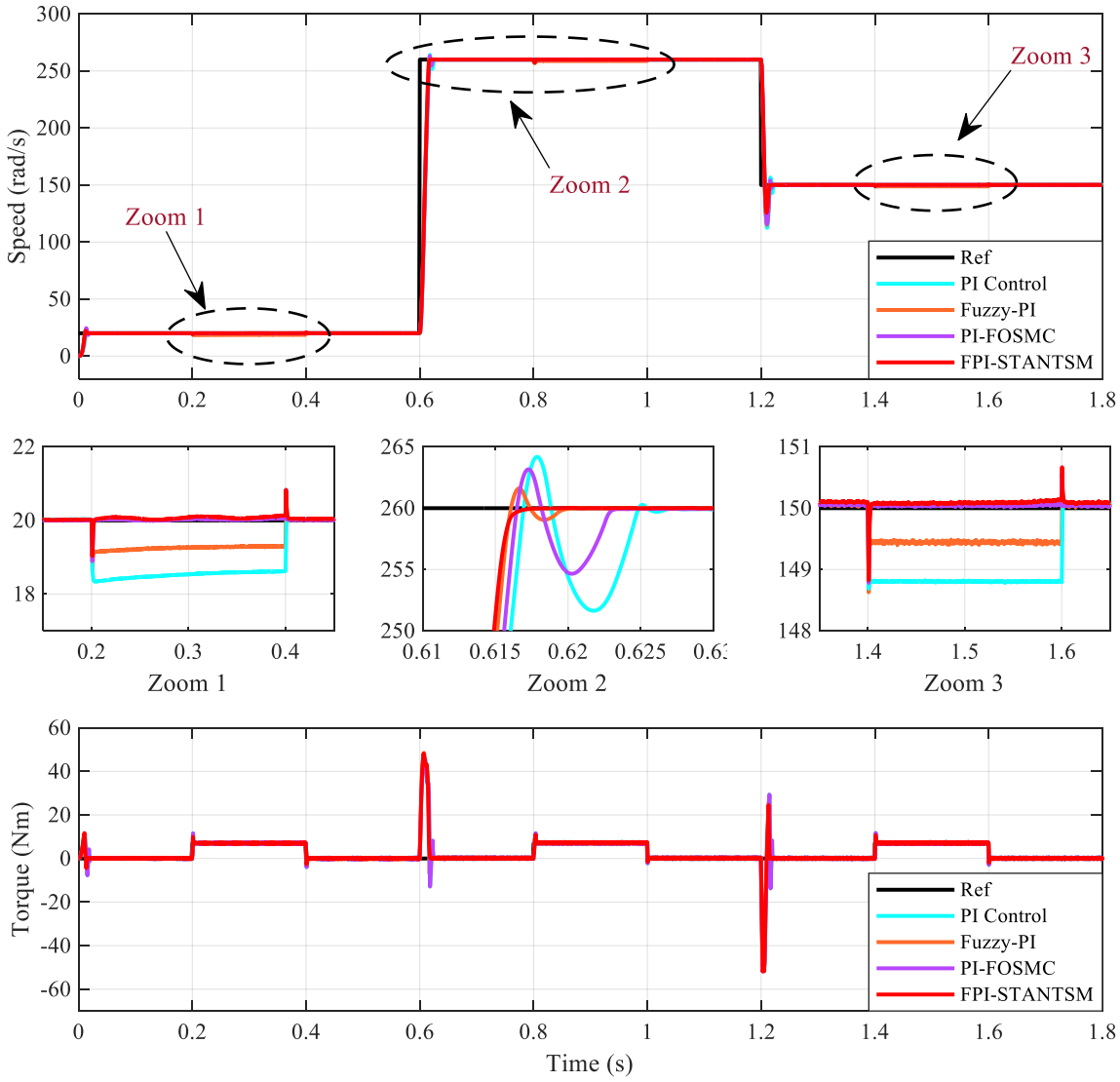

Fig. 6. Performance of PI, Fuzzy-PI, PI-FOSMC and FPI-STANTSMC under the Load Disturbance

5. Conclusion

This paper has presented a novel FPI–STANTSMC control strategy for high-performance induction motor drives. The main contribution lies in unifying three complementary mechanisms within a single framework: (i) fuzzy-PI regulation for adaptive gain tuning and improved steady-state accuracy, (ii) the super-twisting algorithm for continuous control vector with reduced chattering, and (iii) a nonsingular terminal sliding-mode surface to guarantee finite-time convergence without singularities. This integrated design advances beyond existing fuzzy–STA or adaptive NTSMC schemes by simultaneously addressing adaptability, robustness, and precision in the context of IM drives. The proposed controller has been validated under demanding scenarios including variable-speed operation with rated load torque, sudden load disturbances, and significant stator/rotor resistance variations. Comparative simulations confirm consistently superior performance over PI,

fuzzy-PI, and PI-FOSMC controllers, achieving faster settling, negligible overshoot, near-zero steady-state error, and smooth torque dynamics with substantially reduced chattering. These results demonstrate that the proposed approach provides a robust and accurate solution for induction motor drives subject to nonlinearities and parameter uncertainties. Beyond the quantitative improvements, the broader impact of this work is its potential to enhance industrial reliability, reduce mechanical stress, and improve energy efficiency in applications such as manufacturing automation, renewable energy conversion, and electric vehicles. Nevertheless, the hybrid structure introduces higher computational load than classical PI controllers, fuzzy rule base design requires expert knowledge, and the present validation is limited to simulation studies. To address these issues, future work will focus on real-time hardware implementation and hardware-in-the-loop experiments to evaluate practical feasibility. Additional directions include the development of automated fuzzy rule tuning methods to ease controller design, extension to sensorless IM drives, and coordinated control of multi-machine systems for large-scale industrial applications.

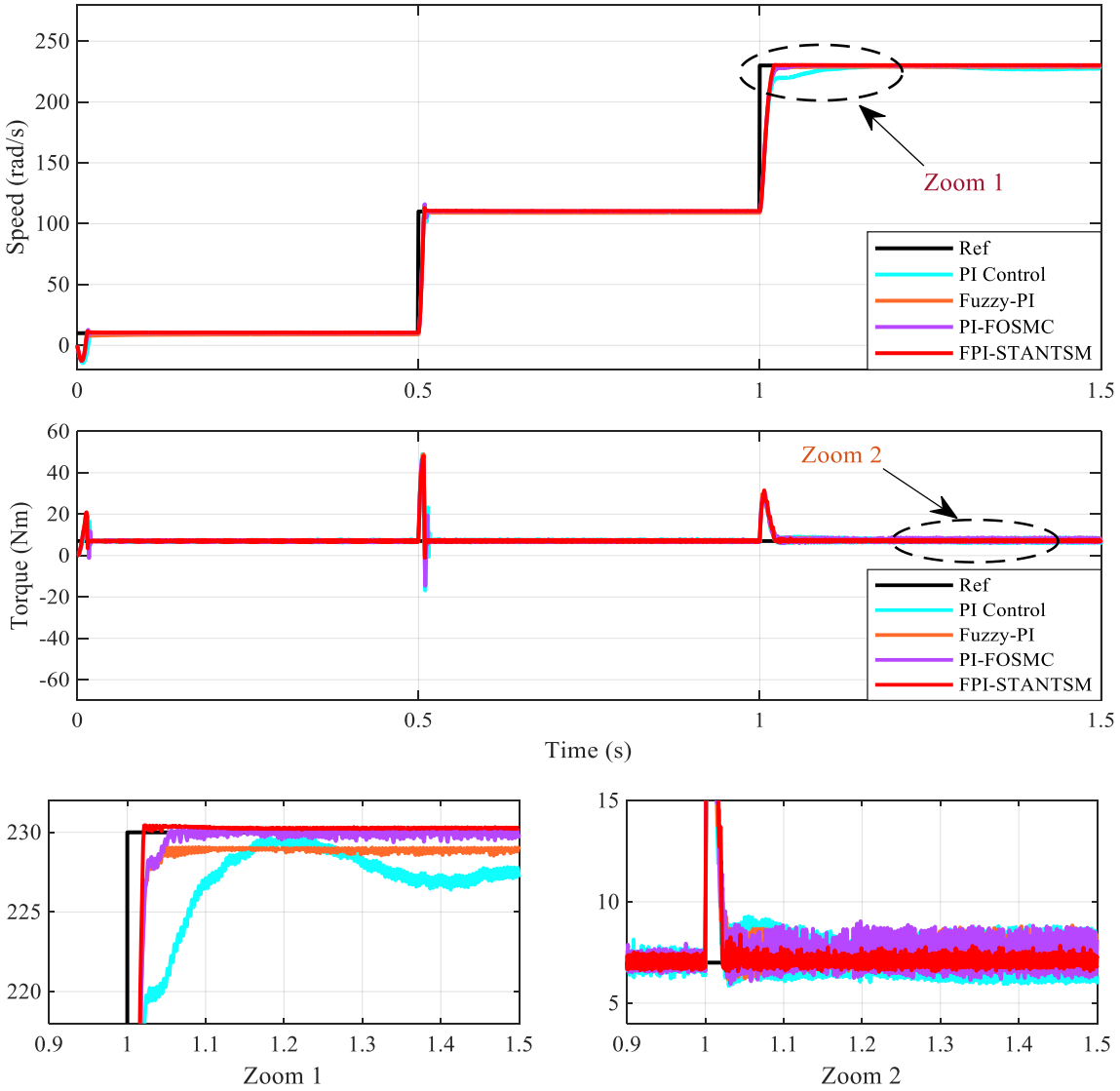

Fig. 7. Performance of PI, Fuzzy-PI, PI-FOSMC and FPI-STANTSMC under Parameter Variations

Author Contribution: All authors contributed equally to the main contributor to this paper. All authors read and approved the final paper.

Funding: This research received no external funding

Conflicts of Interest: The authors declare no conflict of interest.

References

[1] M. A. Azab, "A review of recent trends in high-efficiency induction motor drives," *Vehicles*, vol. 7, no. 1, p. 15, 2025, https://doi.org/10.3390/vehicles7010015.

[2] E. B. Agamloh and A. Cavagnino, "High efficiency design of induction machines for industrial applications," in *Proc. IEEE Workshop Electr. Mach. Design, Control Diagnosis (WEMDCD)*, Paris, France, 2013, pp. 33–46, https://doi.org/10.1109/WEMDCD.2013.6525163.

[3] K.-K. Shyu, F.-J. Lin, H.-J. Lin, and B.-S. Juang, "Robust variable structure speed control for induction motor drive," *IEEE Trans. Aerosp. Electron. Syst.*, vol. 35, no. 1, pp. 215–224, Jan. 1999, https://doi.org/10.1109/7.745693.

[4] J. Wang, F. Wang, Z. Zhang, S. Li, and J. Rodríguez, "Design and implementation of disturbance compensation-based enhanced robust finite control set predictive torque control for induction motor systems," *IEEE Trans. Ind. Informat.*, vol. 13, no. 5, pp. 2645–2656, Oct. 2017, https://doi.org/10.1109/TII.2017.2679283.

[5] J. K. Jain, S. Ghosh, and S. Maity, "Concurrent PI controller design for indirect vector controlled induction motor," *Asian J. Control*, vol. 22, no. 1, pp. 130–142, 2018, https://doi.org/10.1002/asjc.1911.

[6] N. Goel, S. Chacko, and R. Patel, "PI controller tuning based on stochastic optimization technique for performance enhancement of DTC induction motor drives," *J. Inst. Eng. (India) B*, vol. 101, pp. 1–8, 2020, https://doi.org/10.1007/s40031-020-00496-z.

[7] R. Arulmozhiyal and K. Baskaran, "Implementation of a fuzzy PI controller for speed control of induction motors using FPGA," *J. Power Electron.*, vol. 10, no. 1, pp. 65–71, Jan. 2010, https://doi.org/10.6113/JPE.2010.10.1.065.

[8] S. V. Ustun and M. Demirtas, "Optimal tuning of PI coefficients by using fuzzy-genetic for V/f controlled induction motor," *Expert Syst. Appl.*, vol. 34, no. 4, pp. 2714–2720, May 2008, https://doi.org/10.1016/j.eswa.2007.05.029.

[9] N. Mohamad Nordin, N. R. N. Idris, N. Azli, M. Puteh, and T. Sutikno, "Fuzzy-PI torque and flux controllers for DTC with multilevel inverter of induction machines," *Int. J. Power Electron. Drive Syst.*, vol. 5, no. 2, pp. 268–282, 2014, https://doi.org/10.11591/ijpeds.v5i2.6581.

[10] H. Li, B. Song, T. Chen, Y. Xie, and X. Zhou, "Adaptive fuzzy PI controller for permanent magnet synchronous motor drive based on predictive functional control," *J. Franklin Inst.*, vol. 358, no. 15, pp. 7333–7364, Oct. 2021, https://doi.org/10.1016/j.jfranklin.2021.07.024.

[11] S. Chandrasekaran, S. Durairaj, and S. Padmavathi, "Performance evaluation of a fuzzy logic controller-based photovoltaic-fed multi-level inverter for a three-phase induction motor," *J. Franklin Inst.*, vol. 358, no. 15, pp. 7394–7412, Oct. 2021, https://doi.org/10.1016/j.jfranklin.2021.07.032.

[12] H. Li, "Adaptive fuzzy PI controller for permanent magnet synchronous motor drive," *ISA Trans.*, vol. 112, pp. 1–10, Jan. 2021, https://doi.org/10.1016/j.isatra.2020.10.013.

[13] Q. A. Tarbosh, Ö. Aydoğdu, N. Farah, M. H. N. Talib, A. Salh, N. Çankaya, F. A. Omar, and A. Durdu, "Review and investigation of simplified rules fuzzy logic speed controller of high performance induction motor drives," *IEEE Access*, vol. 8, pp. 49377–49394, 2020, https://doi.org/10.1109/ACCESS.2020.2977115.

[14] T. Li, A. Li, and L. Hou, "Improved GOA-based fuzzy PI speed control of PMSM with predictive current regulation," *PLoS One*, vol. 20, no. 1, p. e0318094, 2025, https://doi.org/10.1371/journal.pone.0318094.

[15] W. Bu, S. Guo, Z. Fan, and J. Li, "Improved adaptive PI-like fuzzy control strategy of permanent magnet synchronous motor," *Energies*, vol. 18, no. 2, p. 362, 2025, https://doi.org/10.3390/en18020362.

[16] M. Öztok and E. Dursun, "Application of fuzzy logic control for enhanced speed control and efficiency in PMSM drives using FOC and SVPWM," *Phys. Scr.*, vol. 100, no. 1, p. 015002, 2025, https://doi.org/10.1088/1402-4896/aded49.

[17] W. Cui, Y. Jiang, B. Zhang, and Y. Shi, "Structured neural-PI control with end-to-end stability and output tracking guarantees," *arXiv preprint,* arXiv:2305.17777, 2023, https://arxiv.org/abs/2305.17777.

[18] J. Günther, E. Reichensdörfer, P. Pilarski, and K. Diepold, "Interpretable PID parameter tuning for control engineering using general dynamic neural networks: An extensive comparison," *PLoS One*, vol. 15, no. 12, p. e0243320, 2020, https://doi.org/10.1371/journal.pone.0243320.

[19] W. Cui, Y. Jiang, B. Zhang, and Y. Shi, "Structured Neural-PI Control for Networked Systems: Stability and Steady-State Optimality Guarantees, " *arXiv preprint,* arXiv:2206.00261, 2023, https://doi.org/10.48550/arXiv.2206.00261.

[20] U. Alejandro-Sanjines, A. Maisincho-Jivaja, V. Asanza, L. Lorente, and D. Peluffo-Ordóñez, "Adaptive PI controller based on a reinforcement learning algorithm for speed control of a DC motor," *Biomimetics*, vol. 8, no. 5, p. 434, 2023, https://doi.org/10.3390/biomimetics8050434.

[21] W. Shipman and L. Coetzee, "Reinforcement learning and deep neural networks for PI controller tuning," *IFAC-Pap. Online*, vol. 52, no. 29, pp. 111–116, 2019, https://doi.org/10.1016/j.ifacol.2019.09.173.

[22] P. Ngoc and L. Thuan, "A novel FOC vector control structure using RBF tuning PI and SM for SPIM drives," *Int. J. Intell. Eng. Syst.*, vol. 13, no. 5, pp. 429–440, Oct. 2020, https://doi.org/10.22266/ijies2020.1031.38.

[23] A. Rubaai and P. Young, "EKF-based PI-/PD-like fuzzy-neural-network controller for brushless drives," *IEEE Trans. Ind. Appl.*, vol. 47, no. 6, pp. 2391–2401, Nov.–Dec. 2011, https://doi.org/10.1109/TIA.2011.2168799.

[24] H. Rafia, H. Ouadi, F. Giri, and E. B. Brahim, "Advanced hybrid control for induction motor combining ANN-PID speed controller with neural predictive current regulator based on particle swarm optimization," *Trans. Inst. Meas. Control*, vol. 47, pp. 1–14, 2024, https://doi.org/10.1177/01423312241277246.

[25] N. H. Sahrir and M. A. M. Basri, "Radial basis function network based self-adaptive PID controller for quadcopter: Through diverse conditions," *Int. J. Robot. Control Syst.*, vol. 4, no. 1, pp. 151–173, 2024, https://doi.org/10.31763/ijrcs.v4i1.1261.

[26] N. H. Sahrir and M. A. M. Basri, "Intelligent PID controller based on neural network for AI-driven control quadcopter UAV," *Int. J. Robot. Control Syst.*, vol. 4, no. 2, pp. 691–708, 2024, https://doi.org/10.31763/ijrcs.v4i2.1374.

[27] X. Zeng, "Adaptive PI and RBFNN-PID current decoupling controller for PMSM drive," *Energies*, vol. 15, no. 17, p. 6353, 2022, https://doi.org/10.3390/en15176353.

[28] S. J. Kim, "Model-free RBF neural network intelligent-PID control for quadrotor systems," *Drones*, vol. 8, no. 5, p. 179, 2024, https://doi.org/10.3390/drones8050179.

[29] J. Fei and Y. Chen, "Dynamic terminal sliding-mode control for single-phase active power filter using new feedback recurrent neural network," *IEEE Trans. Power Electron.*, vol. 35, no. 9, pp. 9904–9922, Sep. 2020, https://doi.org/10.1109/TPEL.2020.2974470.

[30] N. Derbel, J. Ghommam, and Q. Zhu, *Applications of Sliding Mode Control*. Singapore: Springer, 2017, https://doi.org/10.1007/978-981-10-2374-3.

[31] P. Proaño et al., "Sliding mode control proposed using a Clegg integrator for speed control of a three-phase induction motor," *Eng. Proc.*, vol. 77, no. 1, Art. no. 8, 2024, https://doi.org/10.3390/engproc2024077008.

[32] L. Fridman and A. Poznyak, "Robust output LQ optimal control via integral sliding modes," *IEEE Trans. Autom. Control*, vol. 56, no. 11, pp. 2699–2704, Nov. 2011, https://doi.org/10.1109/TAC.2011.2159420.

[33] T. Wang, B. Wang, Y. Yu, and D. Xu, "Discrete sliding-mode-based MRAS for speed-sensorless induction motor drives in the high-speed range," *IEEE Trans. Power Electron.*, vol. 38, no. 5, pp. 5777–5790, May 2023, https://doi.org/10.1109/TPEL.2023.3236024.

[34] D. Zhang, J. Hu, J. Cheng, Z.-G. Wu, and H. Yan, "A novel disturbance observer based fixed-time sliding mode control for robotic manipulators with global fast convergence," *IEEE/CAA J. Autom. Sinica*, vol. 11, no. 3, pp. 661–672, Mar. 2024, https://doi.org/10.1109/JAS.2023.123948.

[35] X. Xiong, H. Chen, Y. Lou, Z. Liu, S. Kamal, and M. Yamamoto, "Implicit discrete-time adaptive first-order sliding mode control with predefined convergence time," *IEEE Trans. Circuits Syst. II, Exp. Briefs*, vol. 68, no. 12, pp. 3562–3566, Dec. 2021, https://doi.org/10.1109/TCSII.2021.3070435.

[36] J. Hong, X. Lin, J. Zhang, W. Huang, B. Yan, and X. Li, "Composite sliding mode control with the first-order differentiator and sliding mode observer for permanent magnet synchronous machine," *ISA Trans.*, vol. 145, pp. 78–89, Feb. 2024, https://doi.org/10.1016/j.isatra.2024.02.006.

[37] J. Xie and J. Fei, "Adaptive fuzzy neural super-twisting control of micro gyroscope sensor," *Sci. Rep.*, vol. 14, p. 15632, 2024, https://doi.org/10.1038/s41598-024-76842-8.

[38] S. Ganguly, M. K. Bera, and P. Roy, "Robust tracking and model following controller based on higher order sliding mode control and observation: With an application to MagLev system," *arXiv preprint,* arXiv:2007.05750, 2020, https://arxiv.org/abs/2007.05750

[39] B. Mohapatra, B. Sahu, and S. Pati, "A novel optimally tuned super twisting sliding mode controller for active and reactive power control in grid-interfaced photovoltaic system," *IET Energy Syst. Integr.*, vol. 5, no. 2, pp. 123–132, 2023, https://doi.org/10.1049/esi2.12117.

[40] Z. Kang, X. Lin, Z. Liu, X. Shen, Y. Gao, and J. Liu, "Adaptive generalized super-twisting sliding mode control for PMSM drives," *IEEE Trans. Energy Convers.*, vol. 40, no. 1, pp. 312–322, Mar. 2025, https://doi.org/10.1109/TEC.2025.3590203.

[41] A. Chalanga, S. Kamal, L. M. Fridman, B. Bandyopadhyay, and J. A. Moreno, "Implementation of super-twisting control: Super-twisting and higher order sliding-mode observer-based approaches," *IEEE Trans. Ind. Electron.*, vol. 63, no. 6, pp. 3677–3685, Jun. 2016, https://doi.org/10.1109/TIE.2016.2523913.

[42] R. Seeber and M. Reichhartinger, "Conditioned super-twisting algorithm for systems with saturated control action," *Automatica*, vol. 116, p. 108921, Jun. 2020, https://doi.org/10.1016/j.automatica.2020.108921.

[43] H. Zhang, P. Ran, and Z. Zhang, "PMSM sensorless control based on super-twisting algorithm sliding mode observer with the IAORLS parameter estimations," *Sci. Rep.*, vol. 15, p. 11234, Feb. 2025, https://doi.org/10.1038/s41598-025-04030-3.

[44] J. Liu, J. Zhu, K. Khayati, D. Zhong, and J. Jiang, "Exponential super-twisting control for nonlinear systems with unknown polynomial perturbations," *Sci. Rep.*, vol. 14, p. 20564, 2024, https://doi.org/10.1038/s41598-024-53761-2.

[45] L. Tan, J. Gao, Y. Luo, and L. Zhang, "Super-twisting sliding mode control with defined boundary layer for chattering reduction of permanent magnet linear synchronous motor," *J. Mech. Sci. Technol.*, vol. 35, no. 7, pp. 3219–3227, Jul. 2021, https://doi.org/10.1007/s12206-021-0403-9.

[46] A. Karami-Mollaee, "Higher order sliding mode control of MIMO induction motors: A new adaptive approach," *Mathematics*, vol. 11, no. 21, p. 4567, Nov. 2023, https://doi.org/10.3390/math11214558.

[47] J. A. Moreno, H. Ríos, L. Ovalle, and L. Fridman, "Multivariable super-twisting algorithm for systems with uncertain input matrix and perturbations," *IEEE Trans. Autom. Control*, vol. 67, no. 12, pp. 6716–6722, Dec. 2022, https://doi.org/10.1109/TAC.2021.3130880.

[48] P. Ngoc, "Design of novel STASOSM controller for FOC control of dual star induction motor drives," *Int. J. Robot. Control Syst.*, vol. 4, no. 3, pp. 1059–1074, 2024, https://doi.org/10.31763/ijrcs.v4i3.1443.

[49] S. Ding, Q. Hou, and H. Wang, "Disturbance-observer-based second-order sliding mode controller for speed control of PMSM drives," *IEEE Trans. Energy Convers.*, vol. 38, no. 1, pp. 100–110, Mar. 2023, https://doi.org/10.1109/TEC.2022.3188630.

[50] X. Lin, B. Zhang, S. Fang, R. Xu, S. Guo, and J. Liu, "Adaptive generalized super-twisting sliding mode control for PMSMs with filtered high-gain observer," *ISA Trans.*, vol. 138, pp. 639–649, Mar. 2023, https://doi.org/10.1016/j.isatra.2023.02.008.

[51] H. Benderradji, S. Benaicha, and L. C. Alaoui, "Improved sliding mode control for induction motor based on twisting algorithm," *AIMS Electron. Electr. Eng.*, vol. 9, no. 1, pp. 81–98, Jan. 2025, https://doi.org/10.3934/electreng.2025005.

[52] B. Wang, T. Wang, Y. Yu, and D. Xu, "Second-order terminal sliding-mode speed controller for induction motor drives with nonlinear control gain," *IEEE Trans. Ind. Electron.*, vol. 70, no. 11, pp. 10923–10934, Nov. 2023, https://doi.org/10.1109/TIE.2022.3231248.

[53] T. Wang, B. Wang, Y. Yu, and D. Xu, "Fast high-order terminal sliding-mode current controller for disturbance compensation and rapid convergence in induction motor drives," *IEEE Trans. Power Electron.*, vol. 38, no. 8, pp. 9593–9605, Aug. 2023, https://doi.org/10.1109/TPEL.2023.3277886.

[54] T. Wang, B. Wang, Y. Yu, and D. Xu, "High-order sliding-mode observer with adaptive gain for sensorless induction motor drives in the wide-speed range," *IEEE Trans. Ind. Electron.*, vol. 70, no. 11, pp. 11055–11066, Nov. 2023, https://doi.org/10.1109/TIE.2022.3227272.

[55] Z. Touati, I. Mahmoud, R. E. Araújo, and A. Khedher, "Fuzzy super-twisting sliding mode controller for switched reluctance wind power generator in low-voltage DC microgrid applications," *Energies*, vol. 17, no. 6, p. 1416, 2024, https://doi.org/10.3390/en17061416.

[56] T. Wang, S. Sun, and Q. Chen, "Non-singular terminal super-twisting control of servo systems with backlash," *Sci. Rep.*, vol. 15, p. 5329, 2025, https://doi.org/10.1038/s41598-025-88795-7.

[57] K. Guo, C. Wei, and P. Shi, "Fuzzy disturbance observer-based adaptive nonsingular terminal sliding mode control for multi-joint robotic manipulators," *Processes*, vol. 13, no. 6, p. 1667, 2025, https://doi.org/10.3390/pr13061667.

[58] J. Yan and H. Hu, "Improved non-singular fast terminal sliding mode PMSM control strategy," *PLoS One*, vol. 20, no. 2, p. e0328004, 2025, https://doi.org/10.1371/journal.pone.0328004.

[59] P. C. Krause, O. Wasynczuk, S. D. Sudhoff, and S. Pekarek, *Analysis of Electric Machinery and Drive Systems*, 3rd ed. Hoboken, NJ, USA: Wiley-IEEE Press, 2013, https://doi.org/10.1002/9781118524336.

[60] R. Krishnan, *Electric Motor Drives: Modeling, Analysis, and Control*, 3rd ed. Upper Saddle River (NJ), USA: Prentice Hall, 2013, https://books.google.co.id/books?id=1lgtAQAAMAAJ.